Supplementary Information for

External Surface and Pore Mouth Catalysis in Hydrolysis of Inulin over Zeolites with Different Micropore Topology and Mesoporosity

Su Cheun Oh[1], Thien Nguyendo[1], Yao He[2], Amanda Filie[1], Yiqing Wu[1], Dat T. Tran[3], Ivan C. Lee[3] and Dongxia Liu[1*]

1. Department of Chemical and Biomolecular Engineering in University of Maryland at College Park, Maryland 20742

2. Institute of Clean Energy Utilization, School of Electric Power, South China University of Technology, Guangzhou, 510640, China

3. U. S. Army Research Laboratory, RDRL-SED-E, 2800 Powder Mill Road, Adelphi, MD, 20783, United States

S1. Physicochemical properties of zeolite catalysts used in inulin hydrolysis

The topological properties, graphical representations of pore topology, acidity, textural properties and morphologies of FER, MFI, MOR, BEA, MWW, BEA, PMFI and PMWW zeolite catalysts have been reported in our previous work[1]. Here, these data are simply repeated for completeness of the study. Table S1 summarizes their acidity and textural properties. Table S2 shows the topological properties of these catalysts. The pH values of the zeolite/deionized (DI) water suspensions are shown in Table S3. The pH value was determined from the suspension that consisted of 50 mg of zeolite and 20 mL of deionized (DI) water, resembling the composition used for the inulin hydrolysis study. The DI water had a pH value of 5.94. The addition of zeolite into DI water caused a decrease in pH of the zeolite/water suspension. Overall, the pH values varied in the range of 4.03 – 4.66 across all the studied zeolite/DI water suspensions. The morphologies of these zeolite samples are shown by SEM images in Figure S1.

Table S1. Acidity and porosity characteristics of the medium-pore, large-pore, and mesoporous zeolites used in sucrose hydrolysis reactions.

Zeolite		Si/Al ratio[a]	Brønsted acid sites[b] (mmol/g)	Cumulative pore vol[c] (cc/g)	Micropore vol[d] (cc/g)	BET surface area[e] (m^2/g)	External surface area[f] (m^2/g)
Medium-pore	FER	28	0.617	0.144	0.103	364	61
	MFI	40	0.438	0.199	0.137	466	196
Large-pore	MOR	45	0.258	0.214	0.162	552	87
	MWW	20	0.450	0.196	0.143	597	161
	BEA	19	0.757	0.260	0.160	612	418
	FAU	40	0.108	0.359	0.201	632	245
Mesopore	PMFI	70	0.235	0.349	0.118	530	303
	PMWW	30	0.370	0.359	0.131	694	339

[a] Determined from elemental analysis (ICP-OES, Galbraith Laboratories). [b] Measured from dimethyl ether titration method [2]. [c] Cumulative pore volume determined using Saito-Foley method. [d] Micropore volume determined by t-plot method. [e] Surface area calculated from the multi-point BET model. [f] Determined from t-method.

Table S2. Topology and graphical representation of pore systems of the medium-pore, large-pore, and mesoporous zeolite catalysts used in the sucrose hydrolysis reactions.

Zeolite		Pore structure		Graphical representation of pore topology
		Pore shape	Pore size (nm)	
Medium-pore	FER	8 MR 10 MR	0.35 x 0.48 0.42 x 0.54	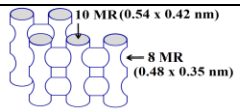
	MFI	10 MR 10 MR	0.51 x 0.55 0.53 x 0.56	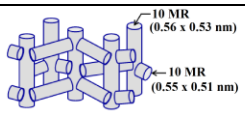
Large-pore	MOR	8 MR 12 MR	0.34 x 0.48 0.65 x 0.7	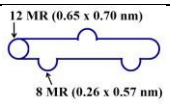
	MWW	10 MR 10 MR supercage side pocket	0.41 x 0.55 0.41 x 0.51 0.71 x 1.82 0.71 d[a] x 0.9 h[b]	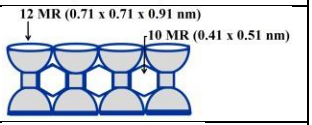
	BEA	12 MR 12 MR	0.56 x 0.56 0.66 x 0.67	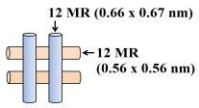
	FAU	12 MR 12 MR	0.74 x 0.74 0.74 x 0.74	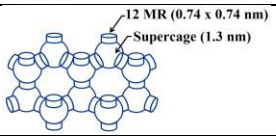
Mesopore	PMFI	10 MR 10 MR mesopore[c]	0.51 x 0.55 0.53 x 0.56 2.8	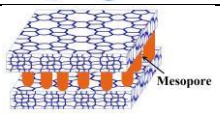
	PMWW	10 MR supercage side pocket mesopore[c]	0.41 x 0.51 0.71 x 1.82 0.71 d[a] x 0.9 h[b] 1.8	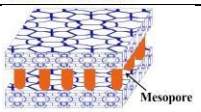

[a] d represents "diameter". [b] h represents "height". [c] The mesopore size was determined from the N_2 adsorption branch by the BJH model.

Table S3. pH of aqueous solution after the addition of zeolite catalyst.

Zeolite/water suspension [a]	FAU	MOR	MFI	MWW	BEA	FER	PMFI	PMWW	DI water
pH	4.66	4.13	4.15	4.77	4.03	4.04	4.33	4.43	5.94

[a] Each zeolie/water suspension contained 20 mL deionized water and 50 mg of zeolite.

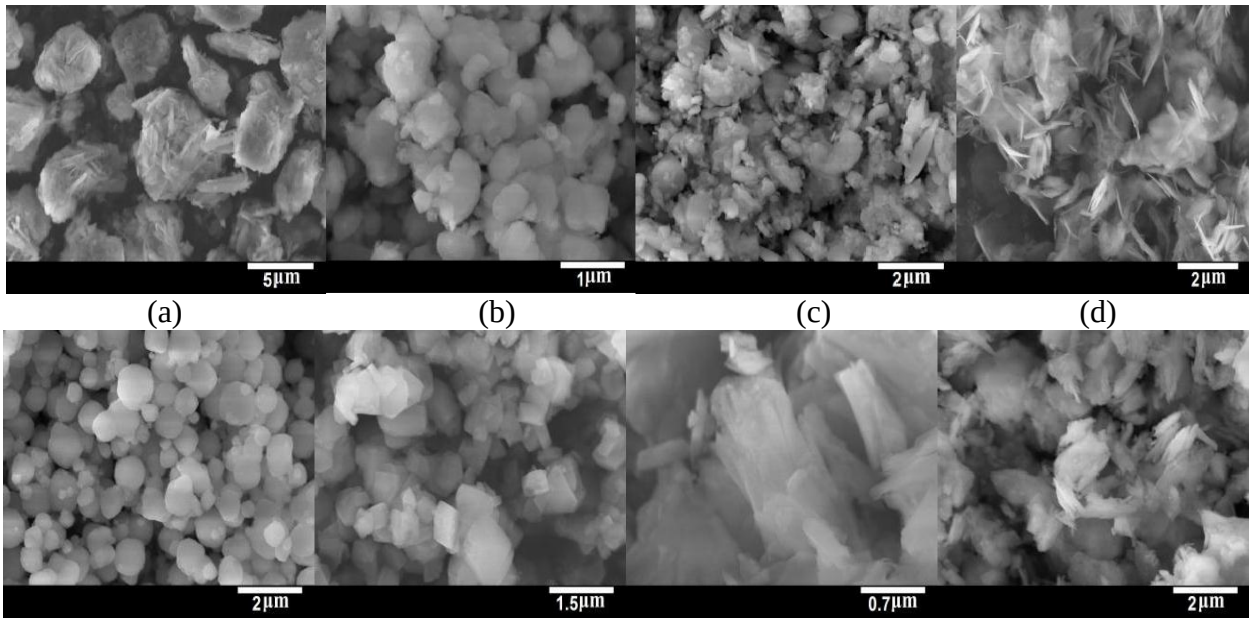

(a) (b) (c) (d)

(e) (f) (g) (h)

Figure S1. SEM images of (a) FER, (b) MFI, (c) MOR, (d) MWW, (e) BEA, (f) FAU, (g) PMFI and (h) PMWW zeolite samples.

S2. Conversion and product selectivity in inulin hydrolysis

S2.1 Conversion and product selectivity versus reaction time over FAU zeolite, in hydrochloric acid solution and in absence of any catalyst

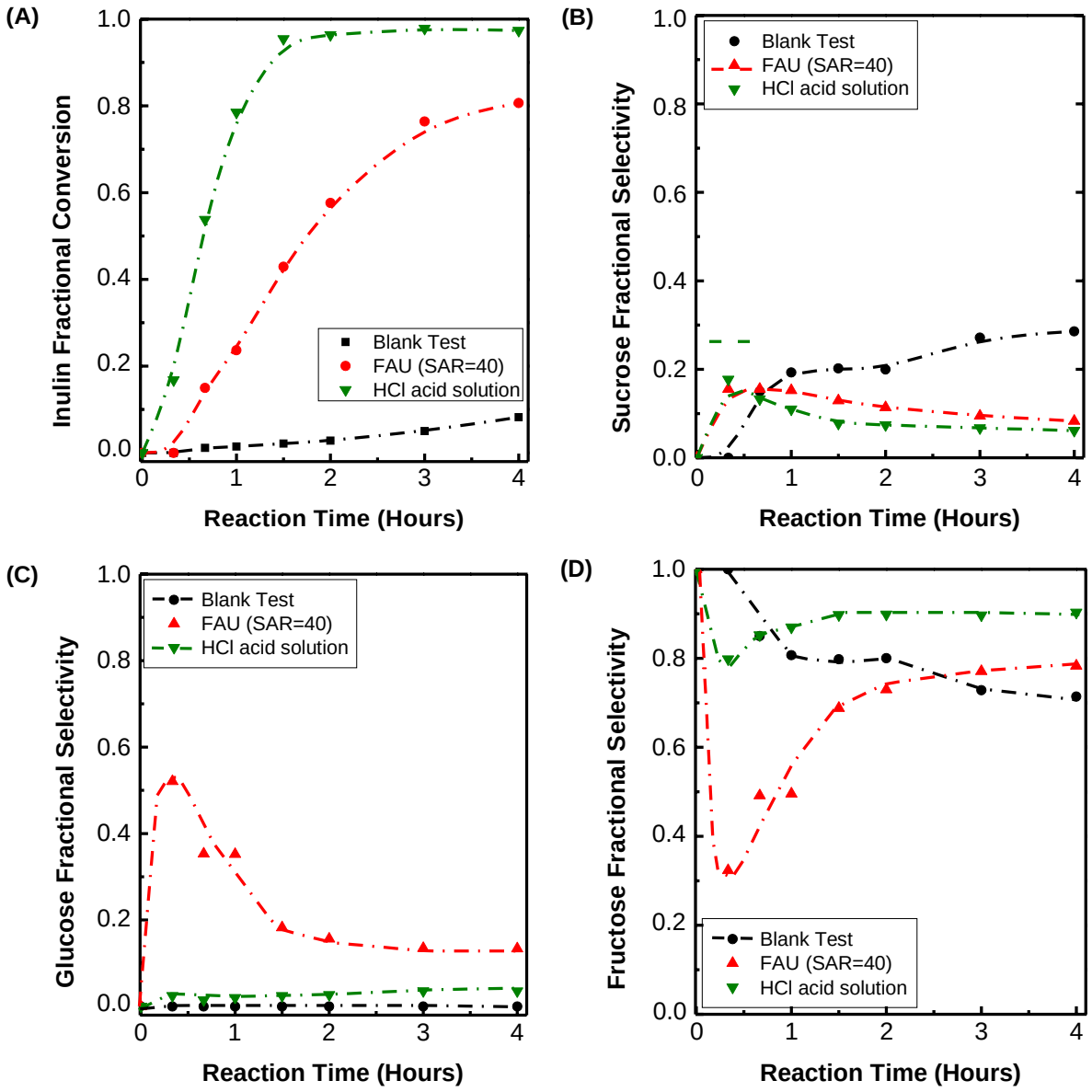

Figure S2. Conversion of inulin (A) and product selectivity ((B) sucrose, (C) glucose and (D) fructose, respectively) in the aqueous solution at 358 K in the presence of hydrochloric acid, FAU zeolite and absence of any catalyst, respectively.

S2.2 Product selectivity versus inulin conversion over zeolite catalysts with different micropore topology

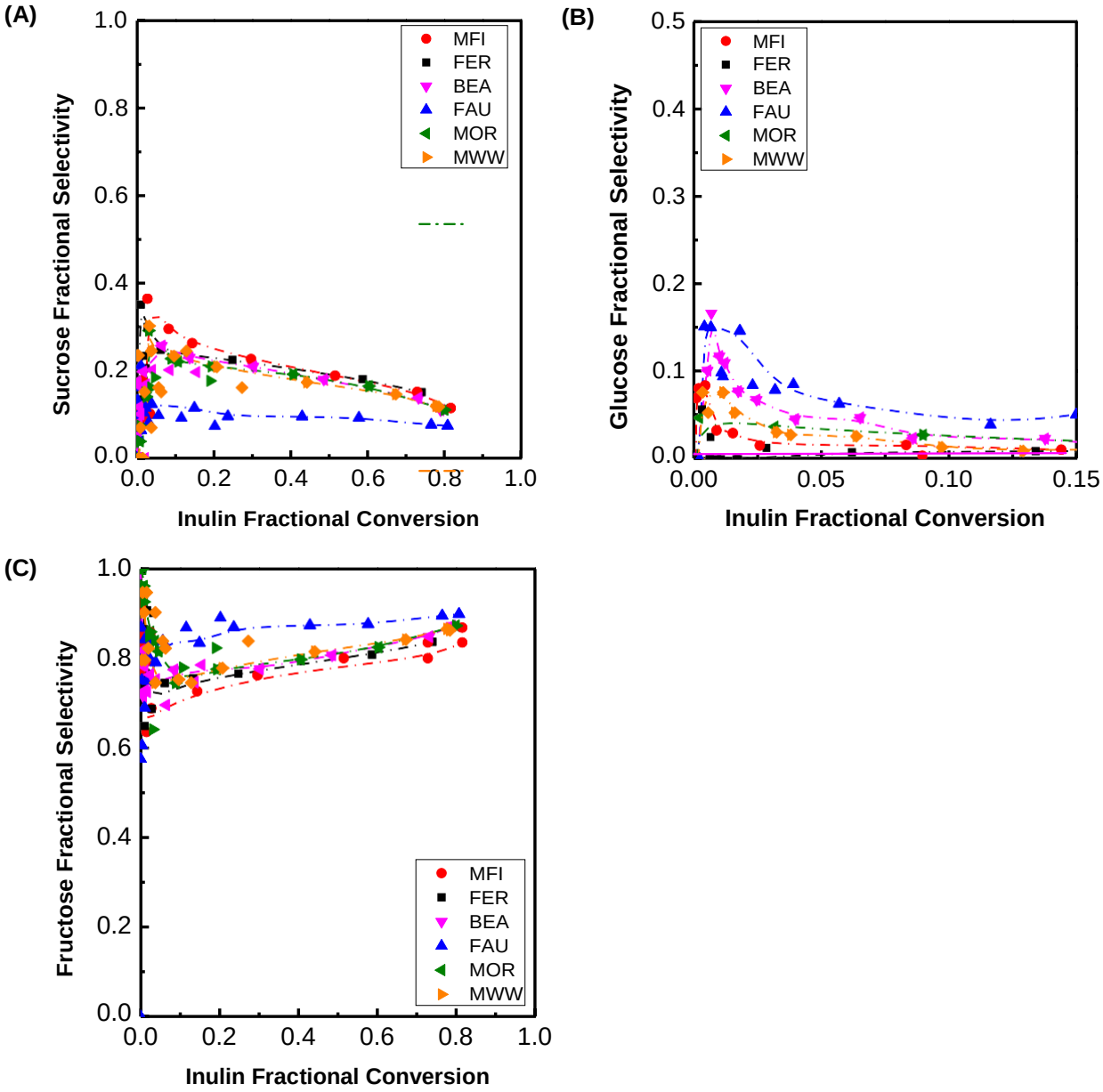

Figure S3. Product selectivity ((A) sucrose, (B) glucose and (C) fructose, respectively) versus inulin conversion in inulin hydrolysis over zeolite catalyst with different micropore topology.

S2.3 Product selectivity versus inulin conversion over zeolite catalysts with different mesoporosity

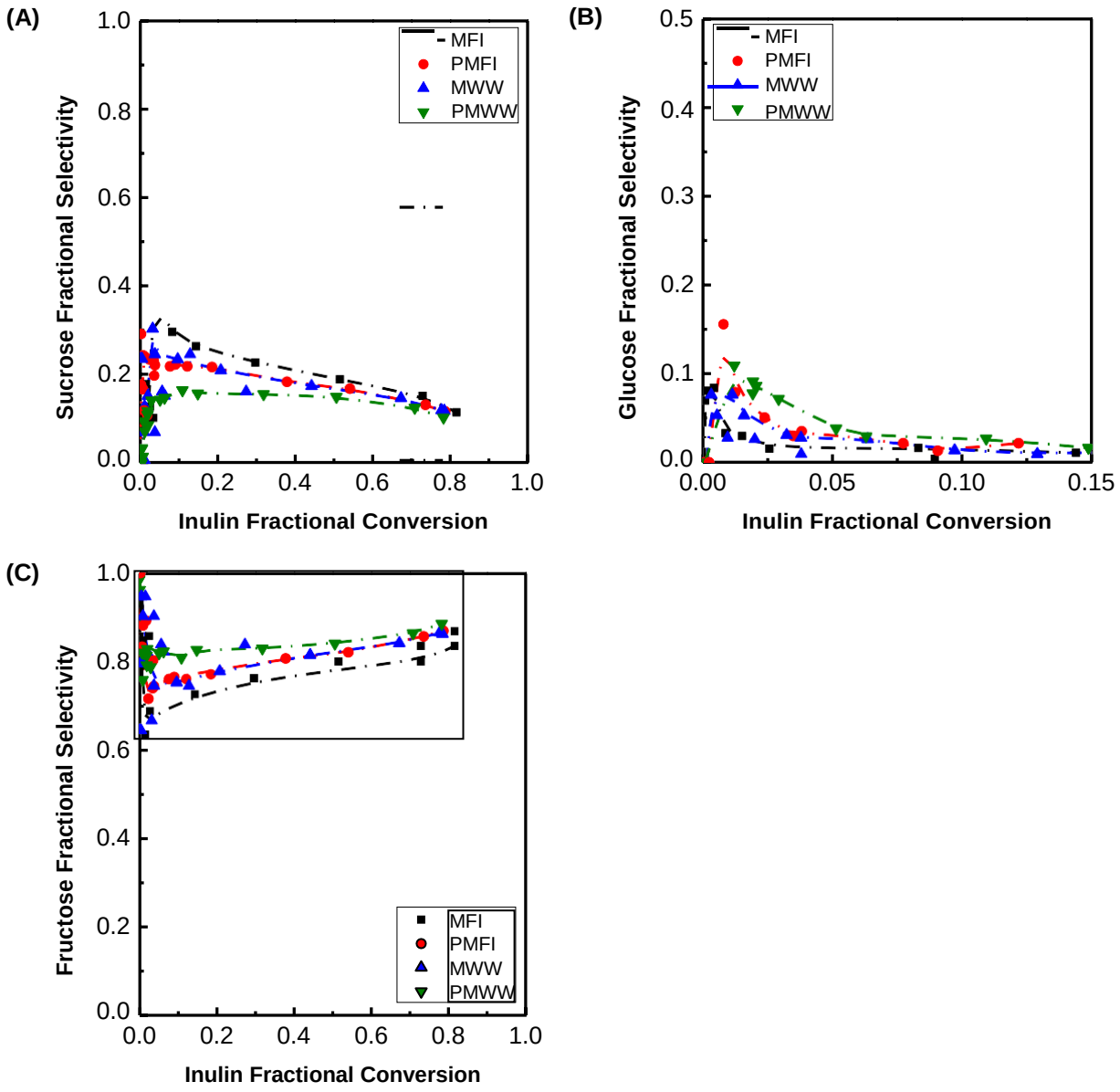

Figure S4. Product selectivity ((A) sucrose, (B) glucose and (C) fructose, respectively) versus inulin conversion over zeolite catalyst with meso-/microporosity.

S2.4 Inulin hydrolysis versus reaction time over zeolites with variable particle sizes and acidities

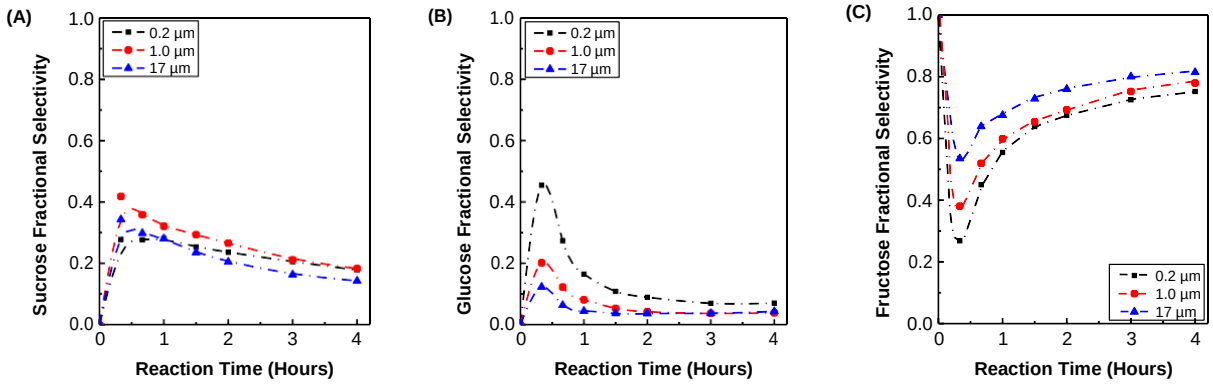

Figure S5. Product selectivity ((A) sucrose, (B) glucose and (C) fructose, respectively) in inulin hydrolysis over MFI with Si/Al ratio of ~30 of different particle sizes. (Lines in the plots are drawn to connect the data points.)

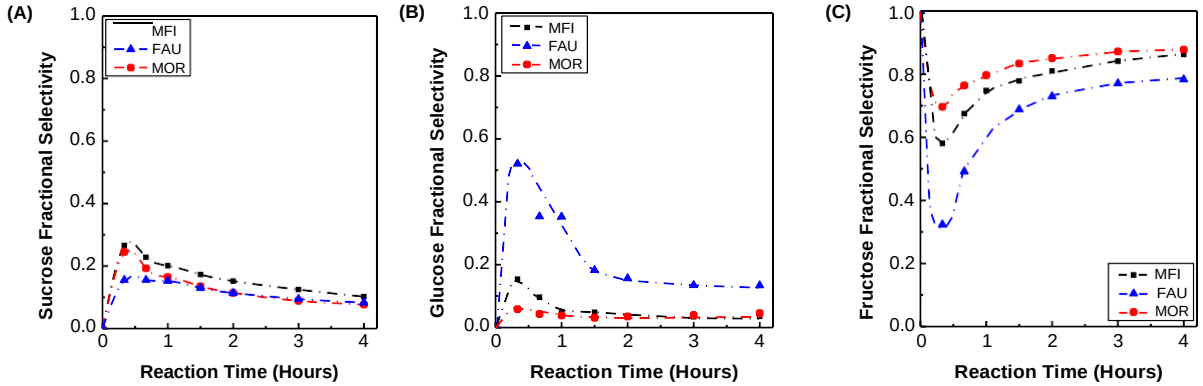

Figure S6. Product selectivity ((A) sucrose, (B) glucose and (C) fructose, respectively) in inulin hydrolysis over MFI, FAU and MOR zeolite catalysts with similar Si/Al ratio and particle size but different micropore topologies. (Lines in the plots are drawn to connect the data points.)

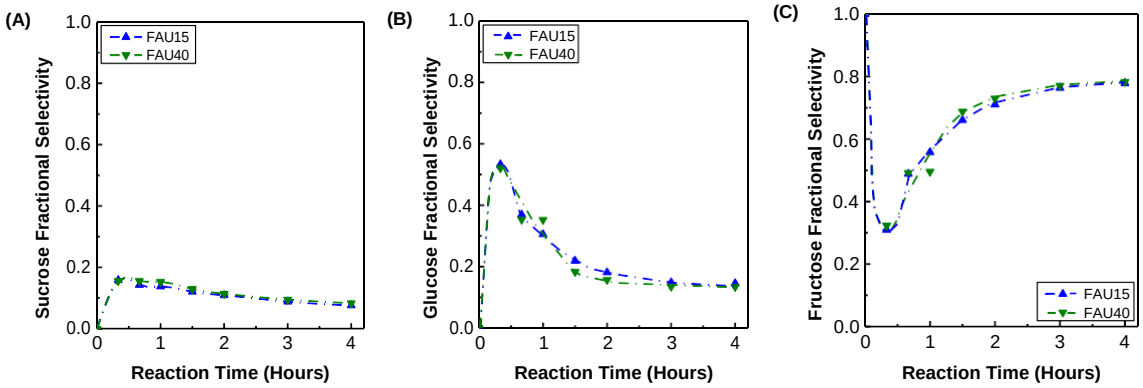

Figure S7. Product selectivity ((A) sucrose, (B) glucose and (C) fructose, respectively) in inulin hydrolysis over FAU zeolite with variable Si/Al ratio. (Lines in the plots are drawn to connect the data points.)

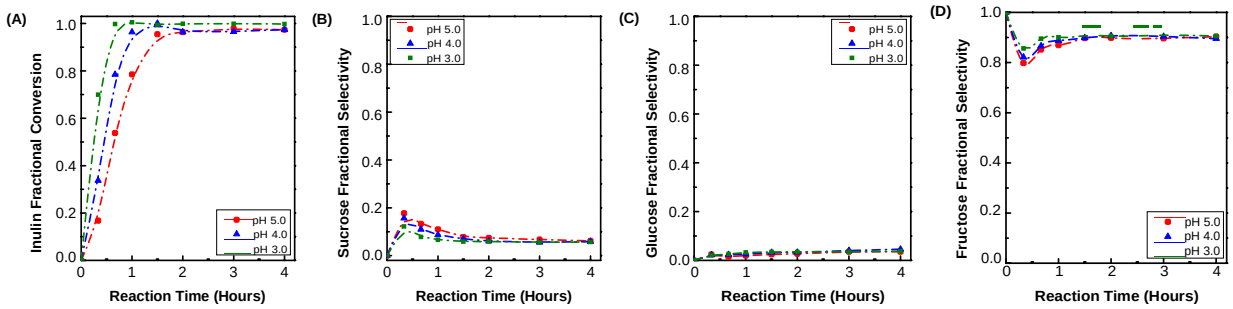

Figure S8. Inulin conversion (A) and product selectivity ((B) sucrose, (C) glucose and (D) fructose, respectively) in inulin hydrolysis over HCl acid solution with variable pH values. (Lines in the plots are drawn to connect the data points.)

S2.5 Inulin hydrolysis over zeolite catalysts in the presence of organic base molecules

The organic base (pyridine or DTBP) poisoning experiment was operated under the same reaction conditions mentioned in the paper except adding pyridine or DTBP into the reactant suspension. Typically, the zeolite catalyst, pyridine or DTBP, and DI water were added to the reactor sequentially, and then the mixture was held at the reaction condition for 3 h before inulin was added. Excess amount of pyridine or DTBP (10 times the total number of acid sites) and 3 h mixing time prior to inulin addition ensured that organic base molecules completely poisoned acid sites that they can reach in the catalysts. Pyridine has a small molecular size which can transport through the zeolite channels (10 MR, 12 MR and mesopores) and can poison all the active Brønsted acid sites in these locations[3-4]. The DTBP molecule is relatively bulky which has restricted capability of accessing to Brønsted acid sites located in micropores (10 MR) in medium sized zeolites[5-6]. It is thus expected that DTBP can poison active sites located in 12 MR and mesopores of the studied zeolite catalysts. Apparently, both pyridine and DTBP can poison the external surface acid sites, but cannot reach the active sites in 8 MR micropores of FER zeolite.

Figure S9 shows the conversion of inulin and product selectivity in the absence of any organic base, in the presence of pyridine and in the presence of DTBP molecules, respectively. The addition of pyridine into the reaction system led to nearly no conversion in inulin over any zeolite catalyst. The addition of DTBP, however, resulted in different degree of inulin conversion loss in different zeolite catalyst. FER and FAU had nearly zero inulin conversion. The first case is due to the small micropores of FER, which limits the reaction solely on the external surface of this zeolite. FAU zeolite has 12 MR micropores, which allows DTBP to reach acid sites inside. Therefore, no inulin conversion was observed in FAU zeolite in the presence of DTBP molecules. For other zeolites (MFI, MWW, BEA, MOR, PMFI and PMWW) zeolites, the inulin conversion was decreased due to the poisoning of the external surface acid sites. At the same time, the product selectivity was slightly shifted to the glucose and sucrose, which supports our conclusion that the pore mouth catalysis promotes the formation of glucose and sucrose products by scission of the terminal sucrosyl-fructosyl and/or glucosyl-fructosyl bonds.

(A) FER zeolite

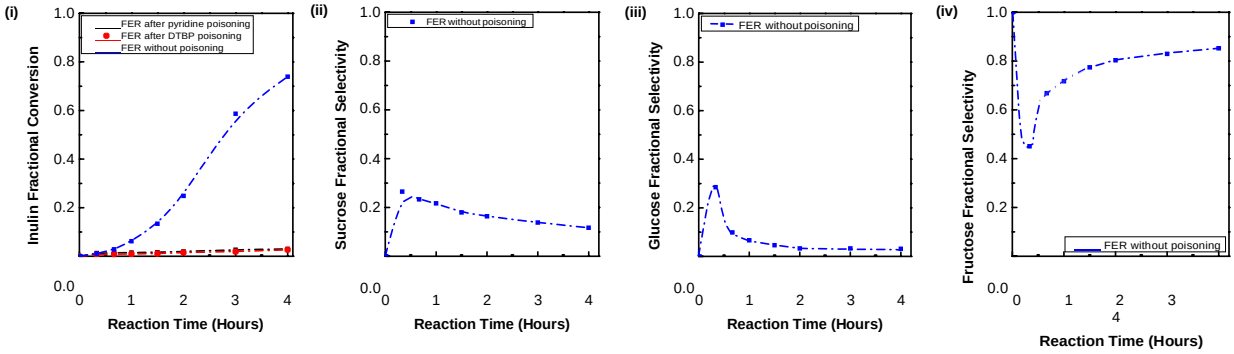

(B) MFI zeolite

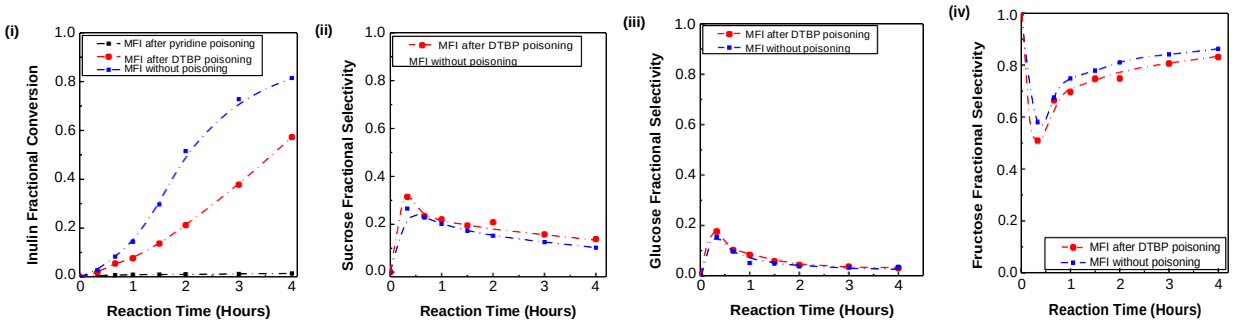

(C) MOR zeolite

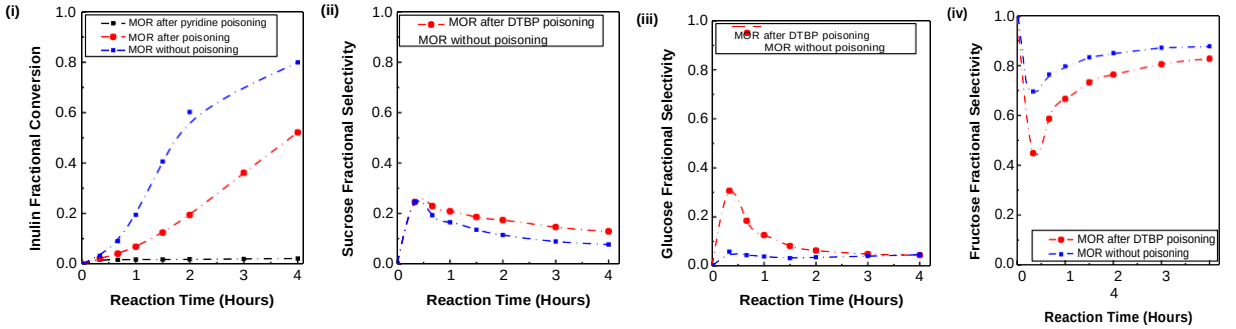

(D) MWW zeolite

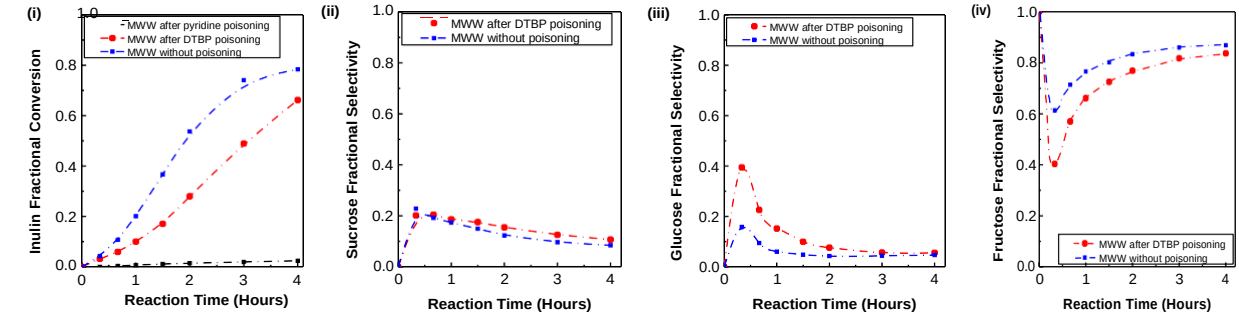

(E) BEA zeolite

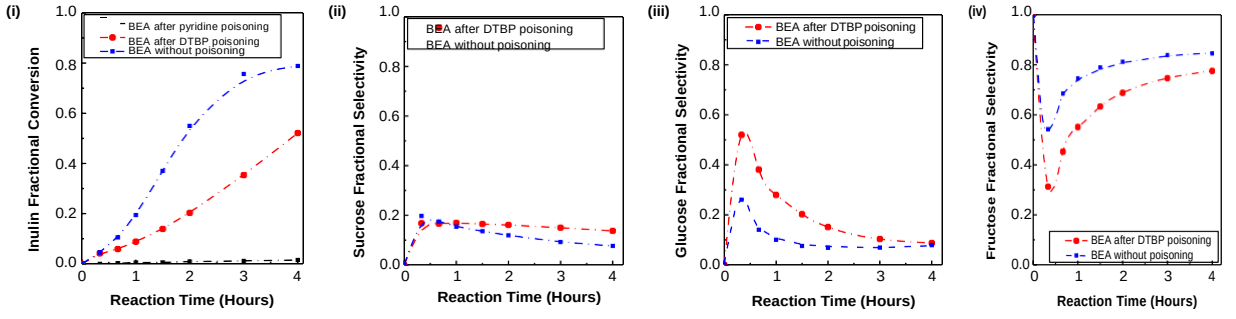

(F) FAU zeolite

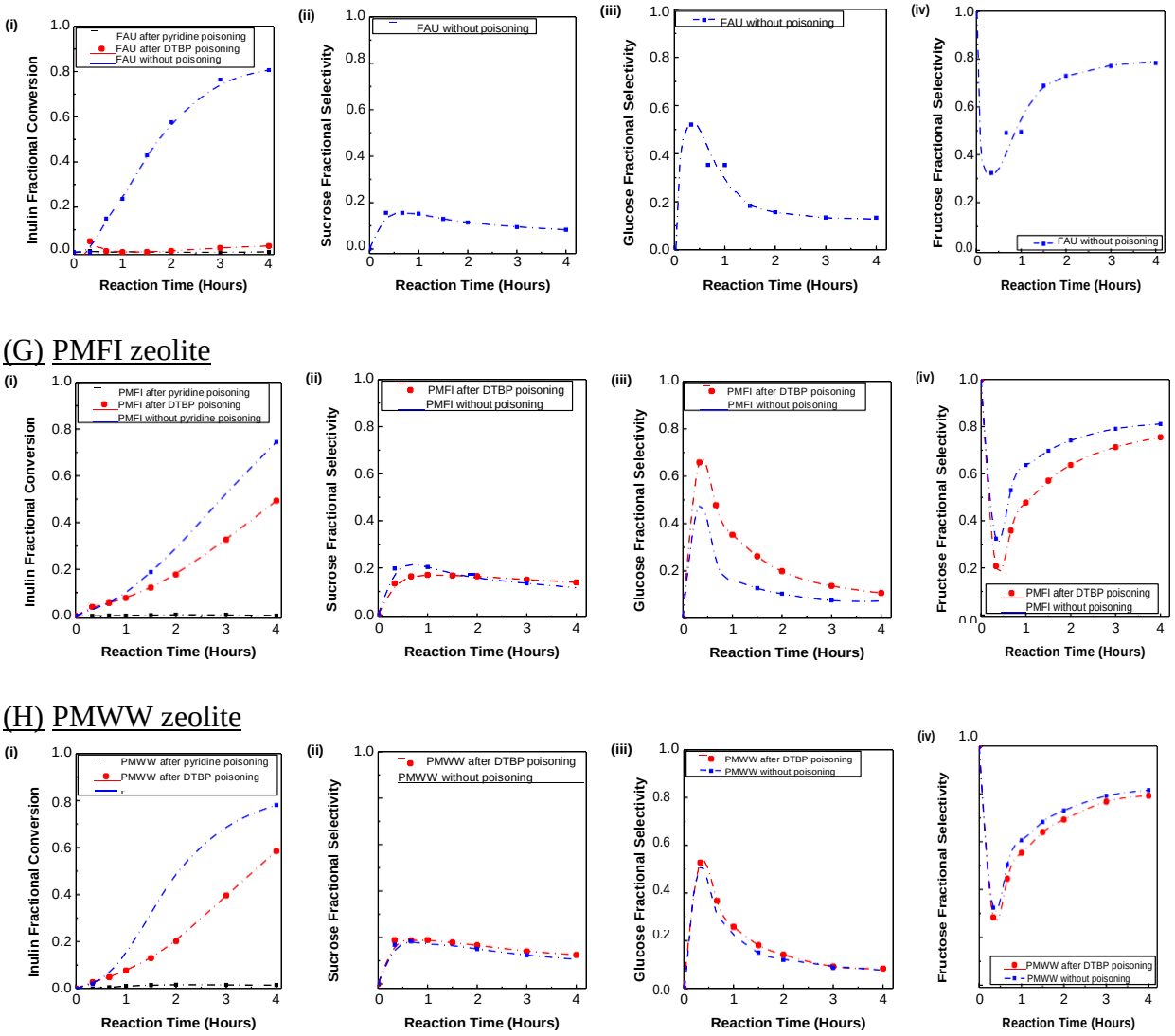

Figure S9. Conversion of inulin and product selectivity versus reaction time over the zeolite catalyst in the presence of pyridine or DTBP organic base molecules.

S3. Derivation of rate equation for inulin hydrolysis over zeolite catalysts

In the proposed reaction network shown in Figure 6 in the main text of the paper, inulin (I) is firstly hydrolyzed to form fructose (F) and truncated inulin chain (I′). This is followed by the breakage of the terminal sucrosyl to fructosyl bond to form sucrose (S) and another shortened inulin chain (I″). The sucrose molecule is further hydrolyzed to form fructose and glucose while the fructosyl to fructosyl bonds internal to the polymer chain in truncated inulin chain are

cleaved to produce fructose molecules. In the present study, the number of sugars in inulin was set as 25 on the basis of the chemical purchased.

S3.1. Derivation of concentration equation for inulin hydrolysis

The rate of inulin disappearance is written as,

$$-\frac{dC_I}{dt} = k_1 C_I \quad \text{(Eq. S3.1)}$$

where C_I is inulin concentration and k_1 is rate constant of inulin consumption. The integral format of Eq. S3.1 is

$$C_I = C_{I,o} e^{-k_1 t} \quad \text{(Eq. S3.2)}$$

where $C_{I,o}$ is the initial inulin concentration. The rate constant for step 1 in the reaction network can be solved based on Eq. S3.2 using the inulin conversion data in the beginning of the reaction.

S3.2 Derivation of truncated inulin concentration equation

The first step in inulin hydrolysis produces one free fructose and truncated inulin chain (I'). The rate equation for I' species is,

$$\frac{dC_I'}{dt} = k_1 C_I - k_2 C_I' \quad \text{(Eq. S3.3)}$$

where C_I' is the concentration of truncated inulin chain and k_2 is the rate constant for hydrolysis of I' to sucrose and I''. Integration of Eq. S3.3 leads to the concentration profile equation for C_I',

$$C_I' = \frac{k_1 C_{I,o}}{(k_2 - k_1)} \left(e^{-k_1 t} - e^{-k_2 t}\right) \quad \text{(Eq. S3.4)}$$

Similarly, the rate equation for I'' species is,

$$\frac{dC_I''}{dt} = k_2 C_I' - k_4 C_I'' \quad \text{(Eq. S3.5)}$$

where C_I'' is the concentration of truncated inulin chain resulted from the hydrolysis of C' and k_4 is the rate constant for hydrolysis of I'' to form fructose in step 4 of this reaction network.

After the substitution of C_I' into Eq. S3.5, $\frac{dC''}{dt}$ can be represented as,

$$\frac{dC_I''}{dt} = k_2 \frac{k_1 C_{I,o}}{k_2 - k_1}(e^{-k_1 t} - e^{-k_2 t}) - k_4 C_I'' \quad \text{(Eq. S3.6)}$$

Eq. S3.6 can be rearranged into,

$$\frac{dC_I''}{dt} + k_4 C_I'' = k_2 \frac{k_1 C_{I,o}}{k_2 - k_1}(e^{-k_1 t} - e^{-k_2 t}) \quad \text{(Eq. S3.7)}$$

Using the integrating factor method, Eq. S3.7 can be solved with boundary condition of $C' = 0_I$ when t = 0.

The concentration profile for C_I' is shown in Eq. S3.8.

$$C_I'' = \frac{k_1 k_2 C_{I,o}}{(k_2 - k_1)}\left[\frac{e^{-k_4 t} - e^{-k_2 t}}{(k_4 - k_2)} + \frac{e^{-k_1 t} - e^{-k_4 t}}{(k_4 - k_1)}\right] \quad \text{(Eq. S3.8)}$$

S3.3 Derivation of sucrose concentration equation

On the basis of the reaction network in Figure 6 in the main text of the paper, sucrose is formed in step 2 and is hydrolyzed to glucose and fructose in step 3. The rate equation for sucrose is,

$$\frac{dC_S}{dt} = k_2 C_I' - k_3 C_S \quad \text{(Eq. S3.9)}$$

where C_S is the sucrose concentration and k_3 is the rate constant of sucrose consumption in step 3. The calculation for rate constant k_3 has been studied in our previous work.[1]

After substitution of Eq. S3.4 into Eq. S3.9, the rate equation for sucrose is written as,

$$\frac{dC_S}{dt} = \frac{k_1 k_2 C_{I,o}}{(k_2 - k_1)}(e^{-k_1 t} - e^{-k_2 t}) - k_3 C_S \quad \text{(Eq. S3.10)}$$

Eq. S3.10 can be rearranged as,

$$\frac{dC_S}{dt} + k_3 C_S = \frac{k_1 k_2 C_{I,o}}{(k_2 - k_1)} (e^{-k_1 t} - e^{-k_2 t}) \quad \text{(Eq. S3.11)}$$

The integrating factor method was applied to solve for sucrose concentration (C_S).

$$C_S = \frac{k_1 k_2 C_{I,o}}{(k^2 - k_1)} [\frac{e^{-k_3 t} - e^{-k_2 t}}{k_3 - k_2} + \frac{e^{-k_1 t} - e^{-k_3 t}}{k_3 - k_1}] \quad \text{(Eq. S3.12)}$$

S3.4 Derivation of glucose concentration equation

Glucose is formed from sucrose hydrolysis in step 3 of the reaction network. The rate equation is,

$$\frac{dC_G}{dt} = k_3 C_S \quad \text{(Eq. S3.13)}$$

where C_G is glucose concentration.

If we substitute C_S in Eq. S3.13 with C_S expression from Eq. S3.12, the rate equation for glucose formation becomes,

$$\frac{dC_G}{dt} = \frac{k_1 k_2 k_3 C_{I,o}}{k_2 - k_1} [\frac{e^{-k_3 t} - e^{-k_2 t}}{k_3 - k_2} + \frac{e^{-k_1 t} - e^{-k_3 t}}{k_3 - k_1}] \quad \text{(Eq. S3.14)}$$

Glucose concentration (C_G) is solved by integrating Eq. S3.14, as shown below,

$$C_G = \frac{k_1 k_2 k_3 C_{I,o}}{k_2 - k_1} [\frac{1}{k_3 - k_2} (\frac{1 - e^{-k_3 t}}{k_3} + \frac{1 - e^{-k_2 t}}{k_2}) + \frac{1}{k_3 - k_2} (\frac{1 - e^{-k_1 t}}{k_1} + \frac{1 - e^{-kt}}{k_3})] \quad \text{(Eq. S3.15)}$$

S3.5 Derivation of fructose concentration equation

The rate equation for fructose is,

$$\frac{dC_F}{dt} = k_1 C_I + k_3 C_S + 22 k_4 C_I'' \quad \text{(Eq. S3.16)}$$

If we substitute the expressions for C_I, C_S and C_I'' into Eq. S3.16, the rate equation for fructose is written as,

$$\frac{dC_F}{dt} = k_1 C_{I,o} e^{-k_1 t} + \frac{k_1 k_2 k_3 C_{I,o}}{k_2 - k_1}\left[\frac{e^{-k_3 t} - e^{-k_2 t}}{k_3 - k_2} + \frac{e^{-k_1 t} - e^{-k_3 t}}{k_3 - k_1}\right] + \frac{22 k_1 k_2 k_4 C_{I,o}}{k_2 - k_1}\left[\frac{e^{-k_4 t} - e^{-k_2 t}}{k_4 - k_2} + \frac{e^{-k_1 t} - e^{-k_4 t}}{k_4 - k_1}\right]$$

(Eq. S3.17)

Fructose concentration (C_F) is solved by integrating Eq. S3.17,

$$C_F = (1 - e^{-k_1 t})C_{I,o} + \frac{k_1 k_2 k_3 C_{I,o}}{k_3 - k_1}\left[\frac{e^{-k_3 t} - 1}{-k_3(k_3 - k_2)} - \frac{e^{-k_2 t} - 1}{-k_2(k_3 - k_2)} + \frac{e^{-k_1 t} - 1}{-k_1(k_3 - k_1)} - \frac{e^{-k_3 t} - 1}{-k_3(k_3 - k_1)}\right]$$
$$+ \frac{22 k_1 k_2 k_4 C_{I,o}}{k_2 - k_1}\left[\frac{e^{-k_4 t} - 1}{-k_4(k_4 - k_2)} - \frac{e^{-k_2 t} - 1}{-k_2(k_4 - k_2)} + \frac{e^{-k_1 t} - 1}{-k_1(k_4 - k_1)} - \frac{e^{-k_4 t} - 1}{-k_4(k_4 - k_1)}\right]$$

(Eq. S3.18)

S3.6 Determination of apparent rate constants for proposed reactions steps

As noted above, the apparent rate constant, k_1, was solved using the data of inulin conversion versus reaction time at the initial stage of inulin hydrolysis. The apparent rate constant, k_3, was calculated on the basis of Arrhenius equation for sucrose hydrolysis that has been published in our previous work.[1] Eq. S3.12 was used to solve for the apparent rate constant k_2 given that k_1, k_3 and $C_{I,o}$ are known.

To quantify the apparent reaction constant, k_4, in the proposed reaction network, a numerical reaction simulation was designed to find the value that best matches the conversion data. Two functions are required, one is used to model the reaction and another is used to fit it to experimental data. Using Matlab R2015a, a function was created to discretize each differential kinetic reaction equation and simulate the reaction given input rate constant values. Relative concentration is stored at each time step. With a total reaction time of 4 hours, a one second time step was shown to be adequate for the model to be time step independent. With the relative

concentrations, the conversion and selectivity are calculated by the function in order to compare the model values with experimental data.

A second function is used to quantify the error between the model and data and subsequently alter the reaction constant k_4 to minimize that error. For each sample measured during the experiment (0.33, 0.67, 1, 1.5, 2, 3, and 4 hours, respectively), the square error was calculated between the experimental conversion and the corresponding model conversion value. The sum of each square error is calculated before using Matlab's built-in minimization function to find a k_4 value that would reduce the error to its lowest possible value. The resulting k_4 best describes the empirical conversion data.

S3.7 Apparent rate constants for proposed reactions steps

Table S4 summarizes the apparent rate constants that were determined from the proposed reaction steps in the inulin hydrolysis reactions.

Table S4. Rate constant of inulin consumption (k_1), rate constant for hydrolysis of I′ to sucrose and I″ (k_2), rate constant of sucrose consumption (k_3) and rate constant for hydrolysis of I″ to form fructose (k_4) at 365 K of inulin hydrolysis reactions over zeolite-based catalyst with different micropore topology and mesoporosity.

Catalyst	k_1 (x 10^{-5} s^{-1})	k_2 (x 10^{-5} s^{-1})	k_3 (x 10^{-5} s^{-1})	k_4 (x 10^{-5} s^{-1})
FER	1.54	23.13	0.0097	9.17
MFI	3.94	24.89	0.16	7.57
MOR	5.06	18.62	0.09	10.11
BEA	4.06	11.58	0.12	4.01
MWW	5.45	18.22	0.34	5.17
FAU	6.55	5.16	4.18	22.42
PMFI	4.92	20.10	0.26	15.67
PMWW	3.70	26.48	0.60	5.32

S4. Assessment of intraparticle and interparticle mass transport limitations.

The Mears Criterion (C_M) was used to assess the interparticle mass transport limitation while Thiele modulus concept was applied to examine intraparticle mass transport limitation in inulin hydrolysis reaction, respectively.[7] External mass transport is negligible when the following criterion (Eq. S4.1) is satisfied at the reaction condition:

$$C_M = \frac{-r_{obs}\rho_b R_P n}{k_c C_{Ab}} < 0.15 \qquad (Eq.\,S4.1)$$

where $-r_{obs}$ is the observed reaction rate (mol kg_{cat}^{-1} s^{-1}), ρ_b is the density of catalyst in reactor (kg_{cat} m_{sol}^{-3}), R_p is the catalyst crystallite radius (m_{cat}), n is the reaction order, k_c is the external mass transfer coefficient (m_{cat} s^{-1}) for inulin reactant, and C_{Ab} is the bulk concentration (mol m_{sol}^{-3}) of inulin (A), respectively.

The density of the catalyst (ρ_b) in the reactor was calculated to be 2.5 x 10^3 kg m_{sol}^{-3} while the reactant concentration (C_{Ab}) was set as 0.62 mol m_{sol}^{-3} in the beginning of the reaction. The reaction order was assumed to be 1. The radius of the zeolite particle was estimated to be 1 x 10^{-6} m, although the zeolite particle size is typically less than this number as shown by the SEM images shown in Figure S1. The external mass transfer coefficient (k_c) is not directly available, but was evaluated using the Frössling correlation (Eq. S4.2) as follows.

$$Sh = 2 + 0.6Re^{1/2}Sc^{1/3} \qquad (Eq.\,S4.2)$$

where Sh is Sherwood number, Re is Reynolds number and Sc is Schmidt number. Eq. S4.2 can be expressed as:

$$\frac{k_c d_P}{D_{AB}} = 2 + 0.6\,[\frac{\rho u d_P}{\mu}]^{1/2}(\frac{\mu}{\rho D_{AB}})^{1/3} \qquad \text{(Eq. S4.3)}$$

where d_P is the catalyst particle diameter (m_{cat}), D_{AB} is diffusion coefficient ($m^2\,s^{-1}$) of inulin in water (B), ρ is the density of the solvent density (kg m^{-3}), u is the fluid velocity (m s^{-1}) and μ is the fluid viscosity (Pa·s), respectively. Tables S5 lists the parameters used for the Mears' criterion calculation as well as the estimated values for the external mass transfer limitation using inulin reactant. The C_M calculated from equations and estimated parameters is ~3.12 x 10^{-5} <<0.15, which indicates the absence of external mass transfer in the reaction.

Table S5. Parameters used in the Mears' criterion for estimating external mass transfer limitations in inulin hydrolysis over zeolite catalyst.

Parameters	*Symbol and unit*	*External mass transfer*
Reaction rate at 365 K	*- r_{obs} (mol kg_{cat}^{-1} s^{-1})* [a]	*1.62 x 10^{-5}*
Catalyst density in reactor	*ρ_b (kg m_{sol}^{-3})* [b]	*2.50 x 10^3*
Solvent density	*ρ (kg m_{sol}^{-3})* [c]	*1.00 x 10^3*
Radius of catalyst particle	*R_p (m_{cat})* [d]	*1.00 x 10^{-6}*
Diameter of catalyst particle	*d_p (m_{cat})*	*2.00 x 10^{-6}*
Inulin concentration in reactor	*C_{Ab} (mol m_{sol}^{-3})* [e]	*0.62*
Velocity of solvent	*u (m_{sol} s^{-1})* [f]	*1.20 x 10^{-4}*
Viscosity of solvent	*μ (Pa·s)* [g]	*3.2 x 10^{-4}*
Reynold number	*Re (unitless)*	*7.50 x 10^{-3}*
Schmidt number	*Sc (unitless)*	*160*
Diffusion coefficient of inulin in water	*D_{AB} (m_{cat}^2 s^{-1})* [h]	*2 x 10^{-9}*
Reaction order	*n (unitless)*	*1*
Mass transfer coefficient	*k_c (m_{cat} s^{-1})* [i]	*2.09 x 10^{-3}*

[a] *Determined from the largest measured rate constant and initial inulin concentration in inulin hydrolysis reaction.*
[b] *Determined by the mass of zeolite catalyst in 20 mL of DI water in inulin hydrolysis reaction.*
[c] *Solvent density was assumed to be the density of DI water.*
[d] *Estimated from the SEM images in Figure S1.*
[e] *The initial inulin concentration was taken as C_{Ab}.*
[f] *Determined by converting magnetic rotation speed (rpm) in reactor to velocity.*
[g] *Viscosity of solvent was assumed to be the viscosity of DI water.*
[h] *Diffusion coefficient of inulin in water was not available in literature. Diffusion coefficient of fibrinogen in water[8] was used to assume the diffusion coefficient of inulin in water.*
[i] *Determined from Eq. S4.3.*

The internal diffusion limitation was checked by estimating the Thiele modulus (∅). It is negligible when the following equation is satisfied at the reaction condition.

$$\emptyset = \frac{-r_{obs}\rho_c {R_P}^2}{D_e C_{As}} = \eta\emptyset^2 \ll 1 \qquad \text{(Eq. S4.4)}$$

where $-r_{obs}$ is the observed reaction rate (mol kg_{cat}^{-1} s^{-1}), ρ_c is the density of zeolite catalyst (kg_{cat} m_{cat}^{-3}), R_p is the catalyst crystallite radius (m_{cat}), D_e is the effective diffusion coefficient of inulin in zeolite (m_{cat}^2 s^{-1}), C_{As} is the surface concentration (mol m_{cat}^{-3}) of inulin in zeolite catalyst and η is the internal effectiveness factor, respectively. The parameters used for the Thiele modulus calculation are listed in Table S6. The $\emptyset$ calculated from Eq. S4.4 was to be ~7.65 x 10^{13} >>1, suggesting that internal diffusion existed seriously in inulin hydrolysis in zeolite catalysts.

Table S6. *Parameters used in estimation of Thiele modulus in inulin hydrolysis over the zeolite catalyst.*

Parameters	*Symbol and unit*	*External mass transfer*
Reaction rate at 365 K	*- r_{obs} (mol kg_{cat}^{-1} s^{-1})* [a]	*1.62 x 10^{-5}*
Density of zeolite catalyst	*ρ_c (kg_{cat} m_{cat}^{-3})* [b]	*1.8 x 10^3*
Radius of catalyst particle	*R_p (m_{cat})* [c]	*1.00 x 10^{-6}*
Effective diffusion coefficient of inulin on zeolite.	*D_e (m_{cat}^2 s^{-1})* [d]	*6.15 x 10^{-20}*
Inulin concentration at catalyst's surface	*C_{As} (mol m_{cat}^{-3})* [e]	*0.62*

[a] *Determined from the largest measured rate constant and initial inulin concentration in the reactor.*
[b] *Density of zeolite catalyst was taken from our previous work[3].*
[c] *Estimated from the SEM images in Figure S1.*
[d] *Effective diffusion coefficient of inulin in zeolite was not available in literature. Effective diffusion coefficient of benzyl alcohol in zeolite catalyst, as estimated in our previous work[9], was taken to estimate the Thiele modulus.*
[e] *Initial inulin concentration was assumed as the inulin concentration at the surface of the catalyst (C_{As}).*

References

1. Y. He, T. C. Hoff, L. Emdadi, Y. Wu, J. Bouraima and D. Liu, *Catal. Sci. Technol.*, 2014, **4**, 3064-3073.

2. D. Liu, A. Bhan, M. Tsapatsis and S. Al Hashimi, *ACS Catal.*, 2011, **1**, 7-17.

3. F. Thibault-Starzyk, I. Stan, S. Abello, A. Bonilla, K. Thomas, C. Fernandez, J. P. Gilson and J. Perez-Ramirez, *J. Catal.* 2009, **264**, 11–14.

4. M. Bevilacqua, T. Montanari, E. Finocchio and G. Busca, *Catal. Today* 2006, **116**, 132–142.

5. J. Macht, C. D. Baertsch, M. May-Lozano, S. L. Soled, Y. Wang and E. Iglesia, *J. Catal.* 2004, **227**, 479–491.

6. D. Farcasiu, R. Leu and A. Corma, *J. Phys. Chem. B* 2002, **106**, 928–932.

7. F. H. Scott, Elements of Chemical Reaction Engineering, 4th ed. (2005), Pg. 839-841.

8. E. L. Cussler, Diffusion: Mass Transfer in Fluid Systems, 2nd ed. (1997), Pg. 112.

9. X. Zhang, D. Liu, D. Xu, S. Asahina, K. A. Cychosz, K. V. Agrawal, Y. A. Wahedi, A. Bhan, S. A. Hashimi, O. Terasaki, M. Thommes, M. Tsapatsis, *Science.*, 2012, **29**, 1684-1687.